Coulomb excitation of Mg-31

Seidlitz, M.; Muecher, D.; Reiter, P.; Bildstein, V.; Blazhev, A.; Bree, N.; Bruyneel, B.; Cederkall, J.; Clement, E.; Davinson, T.

Published in:
Physics Letters B

DOI:
10.1016/j.physletb.2011.05.009

Publication date:
2011

Physics Letters B 700 (2011) 181–186

Contents lists available at ScienceDirect

Physics Letters B

www.elsevier.com/locate/physletb

Coulomb excitation of ^{31}Mg

M. Seidlitz [a,*,1], D. Mücher [a,b,1], P. Reiter [a,1], V. Bildstein [b,c,1], A. Blazhev [a,1], N. Bree [d,1], B. Bruyneel [a,1], J. Cederkäll [e,1], E. Clement [f,1], T. Davinson [g,1], P. Van Duppen [d,1], A. Ekström [e,1], F. Finke [a,1], L.M. Fraile [h,i,1], K. Geibel [a,1], R. Gernhäuser [b,1], H. Hess [a,1], A. Holler [a,1], M. Huyse [d,1], O. Ivanov [d,1], J. Jolie [a,1], M. Kalkühler [a,1], T. Kotthaus [a,1], R. Krücken [b,1], R. Lutter [j,1], E. Piselli [h,1], H. Scheit [k,l,1], I. Stefanescu [d,1], J. Van de Walle [h,m,1], D. Voulot [h,1], N. Warr [a,1], F. Wenander [h,1], A. Wiens [a,1]

[a] Institut für Kernphysik, Universität zu Köln, 50937 Köln, Germany
[b] Physik Department E12, Technische Universität München, 85748 Garching, Germany
[c] Department of Physics, University of Guelph, Guelph ON, N1G 2W1, Canada
[d] Instituut for Kern- en Strahlingsfysica, Katholieke Universiteit Leuven, 3001 Leuven, Belgium
[e] Department of Physics, Lund University, SE-221 00 Lund, Sweden
[f] Grand Accélérateur National d'Ions Lourds (GANIL), 14021 Caen Cedex, France
[g] School of Physics and Astronomy, University of Edinburgh, Edinburgh EH9 3JZ, United Kingdom
[h] ISOLDE, CERN, Physics Department, 1211 Genève 23, Switzerland
[i] Grupo de Física Nuclear, Universidad Complutense, 28040 Madrid, Spain
[j] Department of Physics, Ludwig Maximilian Universität München, 85748 Garching, Germany
[k] Max-Planck-Institut für Kernphysik, 69029 Heidelberg, Germany
[l] RIKEN Nishina Center, RIKEN, Wako, Saitama 351-0198, Japan
[m] Kernfysisch Versneller Instituut, Rijksuniversiteit Groningen, 9747 AA Groningen, Netherlands

ARTICLE INFO

Article history:
Received 10 March 2011
Received in revised form 29 April 2011
Accepted 5 May 2011
Available online 10 May 2011
Editor: V. Metag

Keywords:
Coulomb excitation
ISOL
Reduced transition matrix element
Island of inversion

ABSTRACT

The ground state properties of ^{31}Mg indicate a change of nuclear shape at $N = 19$ with a deformed $J^{\pi} = 1/2^{+}$ intruder state as a ground state, implying that ^{31}Mg is part of the "island of inversion". The collective properties of excited states were the subject of a Coulomb excitation experiment at REX-ISOLDE, CERN, employing a radioactive ^{31}Mg beam. De-excitation γ-rays were detected by the MINIBALL γ-spectrometer in coincidence with scattered particles in a segmented Si-detector. The level scheme of ^{31}Mg was extended. Spin and parity assignment of the 945 keV state yielded $5/2^{+}$ and its de-excitation is dominated by a strong collective M1 transition. Comparison of the transition probabilities of ^{30,31,32}Mg establishes that for the $N = 19$ magnesium isotope not only the ground state but also excited states are largely dominated by a deformed pf intruder configuration.

1. Motivation

Shell structure is one of the most important frameworks for understanding nuclear structure and the properties of atomic nuclei. Recent experimental and theoretical findings indicate that magic numbers are subject to the proton-to-neutron ratio and new magic numbers are revealed when going to more exotic nuclei. Such a new magic number was proposed at $N = 16$ for some nuclei between $Z = 8$ (oxygen) and $Z = 14$ (silicon) [1,2] and confirmed in recent experiments [3]. The shell model modifications and the occurrence of new magic numbers are traced back to the residual nucleon–nucleon interaction. The $(\sigma\sigma)(\tau\tau)$ monopole term of the strongly attractive pairing interaction of protons and neutrons is strongest for $S = 0$ (spin-flip), $\Delta L = 0$ (spin–orbit partner) and $T = 0$ (isospin-flip) [1]. In the case of silicon, protons in the $\pi d_{5/2}$ orbital strongly interact with neutrons in $\nu d_{3/2}$, the $\nu d_{3/2}$ orbital becomes lower in energy, resulting in the classical magic number $N = 20$. By removing protons from the $\pi d_{5/2}$ orbital the residual interaction decreases due to the missing $S = 0$ partner protons and the neutron $d_{3/2}$ orbital is shifted to higher energies. The energy gap to the pf shell becomes smaller, causing a new (sub)shell closure at $N = 16$.

The neutron-rich isotopes of Ne, Na and Mg are located at this transition from a shell closure at $N = 20$ to a shell closure at $N = 16$. Early mass measurements for ^{31,32}Na and ^{31,32}Mg at ISOLDE (CERN) found deviations from the expected values for a closed shell at $N = 20$ [4,5]. Campi et al. suggested a deformed

* Corresponding author.
E-mail address: m.seidlitz@ikp.uni-koeln.de (M. Seidlitz).
[1] For the MINIBALL and REX-ISOLDE Collaboration.

0370-2693/$ – see front matter
doi:10.1016/j.physletb.2011.05.009

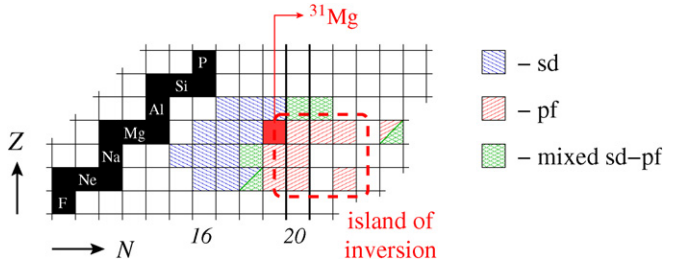

Fig. 1. Location of the "island of inversion" inside the chart of nuclides with recent experimental evidence [9–31]. Nuclides colored in blue show normal *sd* shell structure, whereas nuclides found to have a *pf* intruder ground state are marked in red. Green boxes mean transitional nuclei with a mixed *sd–pf* configuration in the ground state. (For interpretation of the references to color in this figure legend, the reader is referred to the web version of this Letter.)

ground state for these nuclei [6]. Later shell model calculations by Warburton et al. [7] showed that the $1f_{7/2}$ orbital becomes lower in energy, reducing the *sd* shell gap and an anomalous inverted level structure was proposed, which is based on 2-particle 2-hole ($2p2h$) neutron cross shell configurations in the ground state. Recent shell model calculations trace this phenomenon back to the nucleon–nucleon tensor interaction [8]. Investigations in the following nuclei evince that ^{29,30,32}Ne [9–11], ^{30,31}Na [13,14] and $^{31-34,36}$Mg [15–21] are part of this so called "island of inversion" (see Fig. 1). In the neutron-rich magnesium isotopes Coulomb excitation experiments were performed at REX-ISOLDE, CERN with ^{30,32}Mg, showing a normal *sd* shell structure for ^{30}Mg [26]. In contrast the large $B(\mathrm{E2}, 0^+ \rightarrow 2^+)$ value of ^{32}Mg [18,19] demonstrates the strong collectivity of this transition at $N = 20$ and indicates a deformation of the ground state, caused by the highly deformed *pf* intruder state. A shape coexistence of this deformed $0^+_{g.s.}$ and an excited 0^+_2 was observed recently [32].

The $N = 19$ nucleus ^{31}Mg, at the boundary of the island of inversion, was subject of a recent hyperfine structure and β-NMR measurement by Neyens et al. [15]. The ground state spin and parity of ^{31}Mg were determined to be $J^\pi = 1/2^+$ in contradiction to previous β-decay studies that yielded a $3/2^+$ ground state [33]. Maréchal and collaborators performed a complementary β-decay experiment on ^{31}Mg [16,34] and observed very weak feeding to the ^{31}Al ground state ($J^\pi = 5/2^+$) and lowest excited states ($J^\pi = 1/2^+, 3/2^+$). Both observations agree well with the $1/2^+$ ground state of ^{31}Mg. The absence of strong β-decay feeding into the lowest lying $J^\pi = 1/2^+, 3/2^+$ states indicates very different single-particle structures of mother- and daughter-nuclei in agreement with a strong $2p2h$ component in the ^{31}Mg ground state wave function. These experimental results were supported by shell model calculations in the *sd–pf* valence space, reproducing the low-lying level scheme of ^{31}Mg remarkably well for the first time [16]. The ground state and the first excited $3/2^+$ state were found to be largely dominated by $2p2h$ intruder configurations, and ^{31}Mg has to be placed inside the island of inversion. Furthermore, theoretical results on the collective properties of excited states in ^{31}Mg predict a deformed positive yrast band – built on the $1/2^+$ ground state – with a collective transition to a $J = 5/2$ state just below 1 MeV. A corresponding $B(\mathrm{E2}, 5/2^+ \rightarrow 1/2^+) = 127\ e^2\mathrm{fm}^4$ value is given [16]. Additional calculations were done by Kimura [35], which yielded an intruder dominated $5/2^+$ state at 0.89 MeV. The electric quadrupole moment of this strongly deformed and largely collective state was predicted to be $Q = -19.1\ e^2\mathrm{fm}^4$ and $Q_s = -21.6\ e^2\mathrm{fm}^4$, calculated by the AMD + GCM wave function and the rigid rotor approximation, respectively [35].

Three promising candidates for such a $5/2^+$ state are known between 600 keV and 1400 keV [36], but spin and parity assignments are not available from β-decay experiments. The unknown $5/2^+$ state and the predicted collective properties of the first excited positive-parity states in ^{31}Mg motivated a first Coulomb excitation experiment with a ^{31}Mg beam in inverse kinematics at REX-ISOLDE, CERN. The intruder configurations also at higher excitation energy are the subject of this investigation to clarify the placement of ^{31}Mg inside the island of inversion. Reduced transition probabilities, i.e. B(E2) and B(M1) values, will be presented and compared to recent theoretical results in this work.

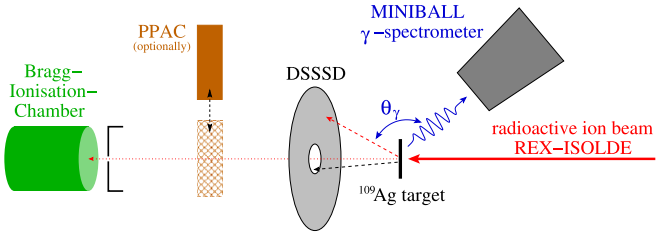

Fig. 2. Schematic view of the experimental MINIBALL setup for the Coulomb excitation of ^{31}Mg at REX-ISOLDE.

2. Experiment

The Coulomb excitation experiment was performed at the REX-ISOLDE facility at CERN [37,38]. The short-lived radioactive ^{31}Mg beam [half-life $t_{1/2} = 232(15)$ ms] was produced by bombarding a 50 g/cm^2 UC_x target with 1.4 GeV protons, provided by the CERN PS Booster, with a maximum intensity of 3.2×10^{13} p/pulse. The pulse repetition time was $n \times 1.2$ s (n integer), at an average of 2.4 s. The produced Mg atoms diffusing out of the heated primary target material were selectively laser ionized by a three-step laser ionization scheme in the Resonance Ionization Laser Ion Source (RILIS) [39]. The extracted 1^+ ions were mass separated by the ISOLDE High Resolution Separator (HRS) and were guided to REX-ISOLDE. Here the ions were first accumulated, cooled, and bunched in a Penning Trap for up to 28.5 ms before injecting into an Electron Beam Ion Source (EBIS) and charge-breeding to high charge states. After an A/q-separation with $A/q = 3.44$ ($q = 9+$) the radioactive ion beam was post-accelerated by the REX linear accelerator and delivered with a final energy of 3.0 MeV/u and an average intensity of 1×10^4 ions/s onto the secondary target inside the highly efficient MINIBALL setup. During the Coulomb excitation experiment two enriched ^{109}Ag targets were used with thicknesses of 1.9 mg/cm^2 and 4.0 mg/cm^2, respectively. The beam on target time added up to 29 hours for the 1.9 mg/cm^2 target and 58 hours for the 4.0 mg/cm^2 target.

The scattered beam and recoiling target nuclei were detected by a CD-shaped 500 μm thick double sided silicon strip detector (DSSSD), consisting of four identical quadrants [40]. Each quadrant comprised 16 annular strips at the front side and 24 radial strips at the back side for identification and reconstruction of the trajectories of the scattered nuclei. The detector covered forward angles between 16.4° and 53.3° in the laboratory system. De-excitation γ-rays following Coulomb excitation of projectile and target nuclei were detected by the MINIBALL γ-spectrometer, consisting of eight triple cluster detectors in close geometry, each containing three 6-fold segmented HPGe crystals [41]. The photopeak efficiency of the array at 1.3 MeV was 8% after cluster addback. The high segmentation of the setup ensured a proper Doppler correction for in-flight γ-ray emission at $v/c \sim 8\%$ by combining the angular information of the γ-ray with the direction and velocity of the scattered beam particle that was detected in coincidence.

Two additional particle detectors were used downstream after the scattering chamber to monitor the position of the beam and

the beam composition, respectively (Fig. 2). A position sensitive parallel plate avalanche counter (PPAC), could be placed right into the beam axis 1.2 m behind the target for measurement of the beam profile in x and y direction [42]. A Bragg ionization chamber close to the beam dump position allowed permanent monitoring of the beam composition in mass A and charge Z [43]. Data were recorded using particle-γ coincidences with a coincidence window of typically 800 ns.

In Coulomb excitation experiments with radioactive ion beams possible beam contaminations have to be carefully investigated, because all beam components contribute to Coulomb excitation of the target material, which is used for normalization. For the extraction of the transition probabilities it was mandatory to monitor and to determine the exact beam composition during the experiment. Different sources of beam contamination were identified: Isobaric contaminants occur by β-decay of the radioactive ^{31}Mg during accumulation and charge breeding at REX-ISOLDE. The isobaric contaminant ^{31}Al, directly produced in the primary ISOLDE target, was surface ionized due to the high temperature of the hot cavity and was not separated completely in the HRS due to the small mass difference ($\Delta m/m = 1/2460$). An additional beam component stemmed from residual argon gas in the REX-Trap and EBIS. After charge breeding, the ^{38}Ar had almost the same A/q ratio ($q = 11+$) and was accelerated together with the ^{31}Mg and ^{31}Al.

The beam composition was carefully monitored during the experiment, using three different techniques: (i) The ratio of laser ionized ^{31}Mg over surface ionized ^{31}Al in the beam was checked by switching the laser on and off periodically every 2.5 hours for about 30 minutes. While the laser was on, ^{31}Mg was elastically scattered into the DSSSD as well as ^{31}Al. When the laser light was blocked, only the surface ionized contaminant was detected. The fraction R of magnesium in the beam was calculated out of the intensities I_{on} with laser on and I_{off} with laser off as $R = (I_{on} - I_{off})/I_{on}$. (ii) The time dependence of the RIB intensity with respect to the proton beam impact on the primary ISOLDE target was analyzed. Due to their fast release out of the primary target [44] and their short lifetime the ^{31}Mg ions showed a high intensity only for the first 800 ms after the proton pulse. For $\Delta t > 800$ ms the contaminants dominated the beam composition. (iii) In addition the exact beam composition was determined with help of the Bragg ionization chamber.

Taking into account the β-decay the accumulated radioactive beam composition of the experiment amounted to 78.9(14)% for ^{31}Mg within a time window of 800 ms after the proton pulse impact, which was applied in the further analysis of the measured γ-intensities. Smaller beam fractions were found to be 17.7(9)% for ^{31}Al and 3.4(5)% for ^{38}Ar.

3. Analysis

Calibration of all DSSSD segments was done with an α-source, containing ^{239}Pu, ^{241}Am, and ^{244}Cm. To calibrate the MINIBALL clusters and to determine their energy dependent efficiency, ^{60}Co and ^{152}Eu sources were mounted onto the target frame at the target position. For Doppler correction, all angles of the cluster detectors had to be known exactly. Therefore an angle-calibration measurement was performed, using Doppler-shifted γ-rays after the neutron pick-up reaction d(^{22}Ne, ^{23}Ne)p.

Coulomb excitation data analysis commenced by selecting scattered ^{31}Mg ions, which were identified by the CD detector (DSSSD). The kinematics of the scattered beam or target particles is clearly separated by the measured correlation of particle energy and scattering angle. In the center-of-mass system a scattering angle range of $\Theta_{CM} = 21.0°$–$66.5°$ is covered. A time window with $\Delta t_p =$ 250 ns between the particle and the γ-ray was applied to select the prompt Coulomb excitation events and to suppress random coincidences from constant room background, i.e. β-decay and bremsstahlung. The prompt Coulomb excitation spectrum for further analysis is particularly clean of any background lines after background subtraction with a long time window $\Delta t_r = 3750$ ns. All observed γ lines are due to Coulomb excitation of either beam or target nuclei.

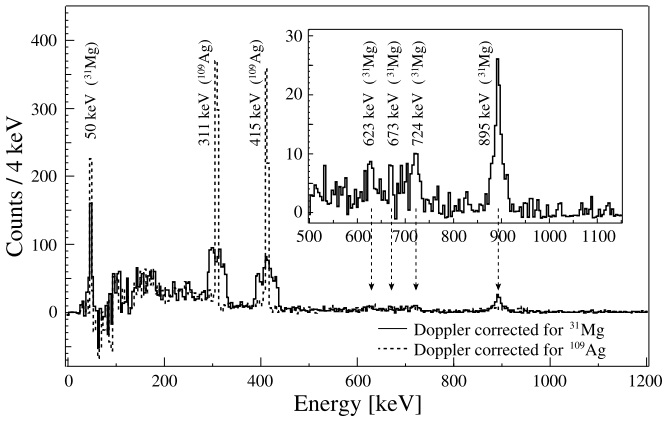

Fig. 3. Doppler corrected and background subtracted γ-spectra in coincidence with beam particles. γ-transitions from the Coulomb excitation of projectile and target nuclei are detected, respectively. Further information is given in the text.

4. Results

Background subtracted γ-ray spectra observed in coincidence with a scattered beam particle in the CD-detector are shown in Fig. 3. Doppler correction was performed for the detected ^{31}Mg projectile and the corresponding recoiling ^{109}Ag target nucleus, respectively. Strong γ-transitions are observed at 311 keV and 415 keV, depopulating Coulomb excited states in ^{109}Ag. The two lines at 50 keV and 895 keV, already observed in β-decay studies of ^{31,32}Na [33,45], are assigned to the transitions of a known excited state at 945 keV in ^{31}Mg. The small Doppler-broadening of the 50 keV line in the spectrum corrected for ^{31}Mg is due to the long half-live of 16(3) ns [33]. The time of flight between target and CD-detector is only 1.7–3.2 ns, thus these γ-rays were emitted at rest after implantation in the detector. There is evidence for three more transitions de-exciting states in ^{31}Mg. Two lines at 623 keV and 673 keV were already established by the β-decay studies as depopulating transitions of an excited state at 673 keV into the $3/2^+$ state at 50 keV and the ground state, respectively. The line at 724 keV was observed for the first time in this work. To identify this γ-transition unambiguously and to place it into the level scheme, information on coincident transitions has been evaluated. Multiple γ-events, that are in prompt coincidence with a detected beam particle, have been sorted into a $\gamma\gamma$-matrix. The known coincident transitions at 895 keV and 50 keV from a $5/2^+ \rightarrow 3/2^+ \rightarrow 1/2^+$ cascade are confirmed by coincidence relations. Despite low statistics of 2–3 counts on a mean background of about 0.02 count/keV, which is in good agreement with the MINIBALL γ-efficiency of ∼10%, the cut spectrum on the 724 keV transition shows clear evidence for coincident γ-rays at 50 keV, 171 keV and 221 keV (see Fig. 4). These transition energies are all known to belong to the low-energy level scheme of ^{31}Mg [33, 45]. The new 724 keV transition can be inserted clearly into the level scheme of ^{31}Mg as de-exciting transition of the 945 keV state, feeding a known $3/2^{(-)}$ state at 221 keV [46,47]. The direct decay of the 945 keV state into the ground state was not observed.

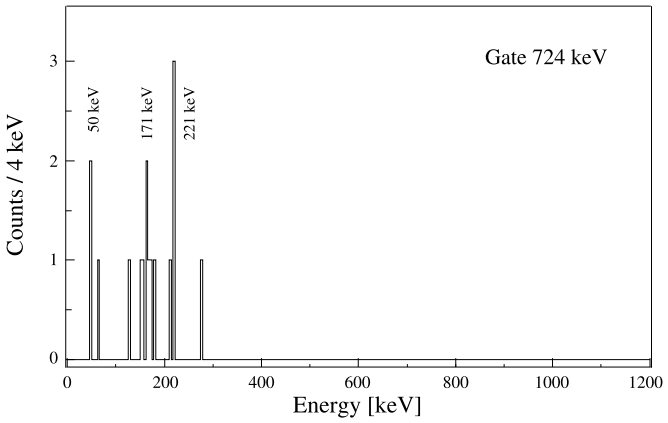

Fig. 4. Prompt γ-coincidences for the 724 keV transition in the Coulomb excitation spectrum of ^{31}Mg. Coincident γ-rays can be observed at 50 keV, 171 keV and 221 keV. Doppler correction was done for the detected ^{31}Mg nucleus.

The measured de-excitation yields of the γ-transitions in ^{31}Mg were used to determine the experimental Coulomb excitation cross sections, which depend on the unknown reduced transition probabilities. These cross sections were normalized to the well-known cross sections for exciting the $3/2^-$ and $5/2^-$ states in the ^{109}Ag target. The fit of the experimental data was performed using the coupled channels Coulomb excitation code GOSIA [48]. The electromagnetic transition matrix elements were fitted using a least squares fit. The calculation takes into account: the energy loss of the projectile in the target material, the angular distribution of the emitted γ-ray, internal conversion coefficients, the position and efficiency of each MINIBALL cluster detector, and an integration over the scattering angle range covered by the CD detector.

Due to the unknown spin and parity values of excited states in ^{31}Mg, different scenarios for the spin and parity of the 945 keV state and different excitation modes were assumed: (i) pure 2-step excitation $1/2^+_{g.s.} \rightarrow 3/2^+ \rightarrow (5/2^+, 7/2^+)$ via M1 and E2, respectively; (ii) E1 excitation to $1/2^-$ or $3/2^-$; (iii) E3 excitation to $5/2^-$ or $7/2^-$; (iv) E2 excitation to $3/2^+$; (v) E2 excitation to $5/2^+$. To limit the valence space of the Coulomb excitation calculation a truncated level scheme of ^{31}Mg was used at this point, containing the following states and connecting transitions that are relevant for excitation of the 945 keV state: the $1/2^+$ ground state, the $3/2^+$ state at 50 keV, and the 945 keV state. Other levels contribute less than 10% to the excitation schemes and were neglected.

First, a possible 2-step excitation into the 945 keV state via the two consecutive transitions with 50 keV and 895 keV, respectively: $1/2^+_{g.s.} \rightarrow 3/2^+ \rightarrow (5/2^+, 7/2^+)$ is clearly excluded. The known $B(\mathrm{M1}, 3/2^+ \rightarrow 1/2^+_{g.s.}) = 0.0190(38)\mu_N^2$ value [36] the M1 excitation implies a M1 Coulomb excitation cross section of 0.05 mb for the 50 keV state. Consequently the next excitation to the 945 keV state, even with a huge E2 matrix element, would yield a nanobarn cross section, which is orders of magnitude less than the measured value of around 160 mb. Therefore the M1 contribution to the excitation is negligible. For the first excitation step a large E2 component of $B(\mathrm{E2}, 1/2^+ \rightarrow 3/2^+) = 80$ W.u. was assumed, which is comparable to the E2 strength of the $0^+ \rightarrow 2^+$ transition in ^{32}Mg. In order to reproduce the measured γ-yields, the second excitation into the 945 keV state would have to have an excitation strength of $B(\mathrm{E2}, 3/2^+ \rightarrow 7/2^+) \approx 400$ W.u. which is much higher than reasonably expected. Consequently scenario (i), a 2-step excitation process, can only play a negligible role in exciting the 945 keV state. Thus the main contribution of the excitation comes from direct excitation from the ground state into the 945 keV state.

In the case of a 1-step excitation via E1 the 945 keV level would have negative parity and the spin would be limited to 1/2 or 3/2. For this assumption GOSIA calculated a reduced excitation probability of $B(\mathrm{E1},\ 1/2^+ \rightarrow 3/2^-_2) = 0.224\ e^2\mathrm{fm}^2$. For de-excitation into the $3/2^+$ state at 50 keV the calculation yielded $B(\mathrm{E1}) = 2.13\ e^2\mathrm{fm}^2$ and $B(\mathrm{M1}) = 127\mu_N^2$ for de-excitation into the $3/2^{(-)}$ state at 221 keV, respectively. For a $1/2^-$ state at 945 keV GOSIA calculated excitation probabilities of the same order. All these values are unreasonably high and scenario (ii) can be excluded. Also an excitation via E3 to a $5/2^-$ or $7/2^-$ state would yield a similar disproportionally huge value of $B(\mathrm{E3})\uparrow > 40\,000\ e^2\mathrm{fm}^6$. Thus a negative parity state, i.e. scenario (iii), can be excluded.

The remaining possibilities to get consistent values for the excitation of the 945 keV state are the scenarios (iv) and (v): direct (1-step) excitation from the ground state via E2 to a $3/2^+$ or a $5/2^+$ state. Now the full known level scheme of ^{31}Mg up to 1 MeV and all known and newly observed transitions were taken into account for the calculation, with adopted B(E1), B(E2), and B(M1) values for the states up to 500 keV [36,46]. Predicted spectroscopic quadrupole moments Q_s and their reduced matrix elements for the $3/2^+$ and $5/2^+$ states [16,35], so called re-orientation matrix elements, were included into the calculation, using [49]

$$Q_s^{\alpha I} = -\sqrt{\frac{16\pi I(2I-1)}{5(I+1)(2I+1)(2I+3)}}M_{\alpha I,\alpha I}(\mathrm{E2}),$$

where $M_{\alpha I,\alpha I}(\mathrm{E2}) = -\langle \alpha I \| \mathfrak{M}(\mathrm{E2}) \| \alpha' I' \rangle$ is the reduced matrix element.

For the 945 keV state the reduced transition probability was calculated to be $B(\mathrm{E2})\uparrow = 182 \pm 17^{+9}_{-13}\ e^2\mathrm{fm}^4$. Both, the $3/2^+$ and $5/2^+$ scenarios coincide within the error bar. The error bar is dominated by the statistical error on the number of counts in the observed γ-transitions and the uncertainty on the beam composition.

De-excitation was investigated using the measured branching ratios of 74(12)% for the 895 keV transition, 24(7)% for the 724 keV transition, and an upper limit of $<$2.6(8)% for the unobserved direct transition to the ground state. Assuming a $3/2^+$ state at 945 keV its de-excitation would have to proceed via E2 + M1 transitions to the ground state and the $3/2^+$ state at 50 keV, respectively. The investigated branching ratios yield a ground state transition via M1/E2 with a reduced transition probability that is hindered by a factor of about 10^{-4} compared to the 895 keV transition. This is very unlikely due to the similar $2p3h$ configuration of the ground state and the first $3/2^+$ excited state at 50 keV [16]. Thus, scenario (iv), i.e. a $3/2^+$ state at 945 keV can be rejected.

The only remaining possibility is that the 945 keV is a $5/2^+$ state (scenario (v)). Assuming a pure E2 transition to the 50 keV state would imply an unreasonably high B(E2) value of about 2700 $e^2\mathrm{fm}^4$ to reproduce the measured intensities. Thus de-excitation to the 50 keV state proceeds via a strong M1 transition with a calculated transition probability range of $B(\mathrm{M1})\downarrow = 0.1 \ldots 0.5\mu_N^2$. These limits depend mostly on the multipole mixing ratio δ of the transition and its absolute E2 strength. The additional de-excitation to the $3/2^{(-)}$ state at 221 keV had to proceed via an E1 transition with $B(\mathrm{E1}) > 8.9 \times 10^{-4}\ e^2\mathrm{fm}^2$.

For the 673 keV state, which is a $3/2^+_2$ state with a $0p1h$ configuration [47], the analysis yielded a reduced transition probability of $B(\mathrm{E2}, 1/2^+ \rightarrow 3/2^+_2) = 21(8)\ e^2\mathrm{fm}^4$. Assuming purely E2 de-excitation from this state as well, the calculation gives $B(\mathrm{E2}) = 11(5)\ e^2\mathrm{fm}^4$ and $B(\mathrm{E2}) = 24(12)\ e^2\mathrm{fm}^4$ for the 673 keV and 623 keV transitions, respectively. The B(E2) value of the 50 keV transition could not be determined due to feeding and a complex, non-uniform efficiency for these 50 keV γ's in the MINIBALL detectors.

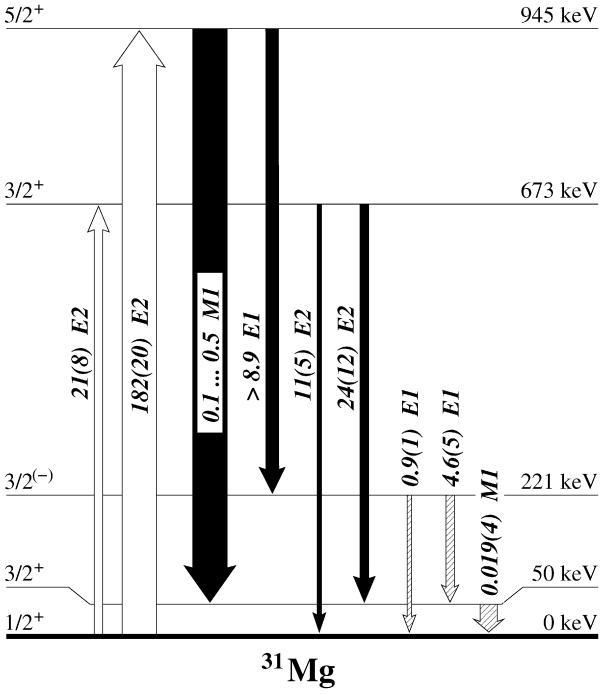

Fig. 5. Measured reduced transition probabilities for ^{31}Mg. B(E2) values are given in e^2fm^4, B(E1) in 10^{-4} e^2fm^2, and B(M1) in μ_N^2. Transition probabilities for the shaded transitions of the levels below 500 keV are taken from [36,46].

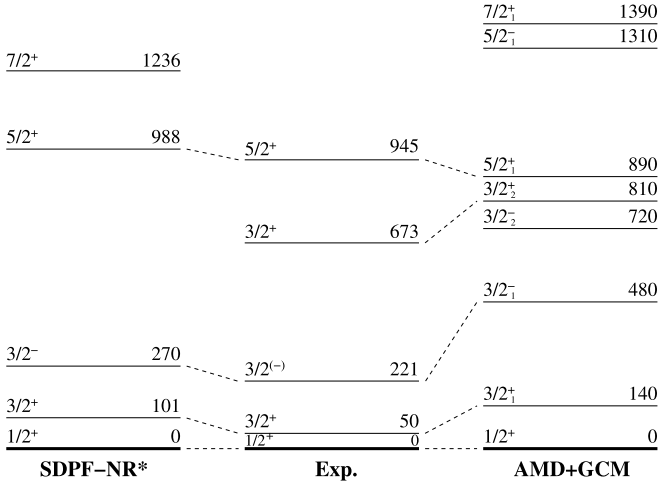

Fig. 6. Level scheme of ^{31}Mg, as it was extracted from the Coulomb excitation data (middle), compared to recently published shell model calculations [16] (left) and AMD + GCM calculations [35] (right). Excitation energies are given in keV.

All reduced transition probabilities that were deduced in this experiment are presented in Fig. 5. For the first time a clear spin and parity assignment was done for the 945 keV state. This $5/2^+$ state is part of a strong collective $K^\pi = 1/2^+$ band in ^{31}Mg.

5. Discussion

The measured level scheme and reduced transition probabilities of ^{31}Mg are compared to results from recently published calculations [16,35]. Both publications predicted a $5/2^+$ state at 988 keV [16] and 0.89 MeV [35], respectively, which is in very good agreement with the present results of the 945 keV state in this work (see Fig. 6). Additionally, the 673 keV state is the $3/2^+_2$ state and the head of the $K^\pi = 3/2^+$ band with a dominant spherical $0p1h$ configuration [47,35]. A reduced coupling to the deformed $2p3h$ ground state configuration is in very good agreement with a less collective transition with $B(\mathrm{E2}, 1/2^+ \to 3/2^+_2) = 21(8)\ e^2\mathrm{fm}^4$ observed in this experiment.

The measured properties of the 945 keV state agree well with the predicted $5/2^+$ state of the positive-parity yrast band in ^{31}Mg. Due to its predicted dominant $2p3h$ configuration the $5/2^+$ state has a strong coupling to the deformed ground state with $B(\mathrm{E2}, 1/2^+ \to 5/2^+) = 182(20)\ e^2\mathrm{fm}^4$. Combined with the $1/2^+$ ground state and the first excited $3/2^+$ state at 50 keV these states form a positive parity yrast band with $K = 1/2$, connected by almost pure M1 transitions. Measured $B(\mathrm{M1}, 5/2^+ \to 3/2^+) = 0.1 \ldots 0.5 \mu_N^2$ and $B(\mathrm{M1}, 3/2^+ \to 1/2^+) = 0.019(4)\mu_N^2$ [36] values agree well with shell model calculations done by Maréchal [16], that yield $B(\mathrm{M1}, 5/2^+ \to 3/2^+) = 0.38\mu_N^2$ and $B(\mathrm{M1}, 3/2^+ \to 1/2^+) = 0.06\mu_N^2$, respectively (see Table 1). For electric quadrupole transitions the shell model calculations do not reproduce the measured values. With $B(\mathrm{E2}, 5/2^+ \to 1/2^+) = 127\ e^2\mathrm{fm}^4$ [16] it is in fact a factor of 2 bigger than the result of the present measurement, that gives $B(\mathrm{E2}) = 61(7)\ e^2\mathrm{fm}^4$.

According to the rigid rotor approximation calculations in [35] another comparison with theory is done by assuming a purely rotational $K = 1/2$ band in ^{31}Mg, given by the sequence $1/2^+ - 3/2^+ - 5/2^+$. For transitions within such a rotational band the reduced transition probability is linked to the intrinsic quadrupole moment Q_0 by [49]

$$B(\mathrm{E2}, I_i \to I_f)_{\mathrm{rot}} = \frac{5}{16\pi} e^2 Q_0^2 \left| \langle I_i 2 K 0 | I_f K \rangle \right|^2 .$$

For the $5/2^+ \to 1/2^+$ transition we get $B(\mathrm{E2})_{\mathrm{rot}} = 69\ e^2\mathrm{fm}^4$ and $B(\mathrm{E2})_{\mathrm{rot}} = 114\ e^2\mathrm{fm}^4$, calculated with predicted quadrupole moments from shell model and rigid rotor approximation calculations, respectively [16,35]. The result from shell model calculations is in reasonable agreement with the experimental result (see Table 1), whereas the rigid rotor approximation yields a transition strength that is too high by a factor of more than 1.8.

The deduced excitation probability $B(\mathrm{E2}, 1/2^+ \to 5/2^+) = 182(20)\ e^2\mathrm{fm}^4$ can be compared to the $0^+ \to 2^+$ E2 strengths in the neighboring even–even magnesium isotopes ^{30,32}Mg. While the excitation B(E2) values always strongly depend on the different spins of the initial (ground) states, the transition strengths of the de-excitation process will be compared instead. For ^{32}Mg the experimental results, i.e. B(E2) values, were discussed by [19], including possible feeding contributions. An E2 strength of $B(\mathrm{E2}, 2^+ \to 0^+) = 89(11)\ e^2\mathrm{fm}^4$ is reported without a correction for feeding, and $B(\mathrm{E2}, 2^+ \to 0^+) = 66(9)\ e^2\mathrm{fm}^4$ includes a correction for feeding from a higher lying state [19], which is consistent with [50]. The new $B(\mathrm{E2}, 5/2^+ \to 1/2^+) = 61(7)\ e^2\mathrm{fm}^4$ of ^{31}Mg compares well with the feeding corrected $B(\mathrm{E2}, 2^+ \to 0^+) = 66(9)\ e^2\mathrm{fm}^4$ of ^{32}Mg [19], and exceeds the $B(\mathrm{E2}, 2^+ \to 0^+) = 48(6)\ e^2\mathrm{fm}^4$ of ^{30}Mg [26]. This result establishes that deformed pf intruder configurations exist for the ground and low lying states already at $N = 19$, including a sequence of collective rotational states.

6. Summary

To summarize, we have investigated Coulomb excitation of the unstable odd-N nucleus ^{31}Mg. The properties of a positive-parity yrast band with $K = 1/2$, built on the $1/2^+$ ground state are in good agreement with a $5/2^+$ state at 945 keV. The determined B(E2) and B(M1) values support this assumption. The increased collectivity is well described by the deformed Nilsson model for excited states in ^{31}Mg. Finally, the quadrupole moment supports

Table 1
Reduced transition probabilities of the positive-parity $K = 1/2$ yrast band in ^{31}Mg, compared to recent theoretical predictions. $B(\mathrm{E2})$ values are given in $e^2\mathrm{fm}^4$, $B(\mathrm{M1})$ in μ_N^2. For more details see text.

$I_i \to I_f$	$B(\mathrm{E2})_{\mathrm{exp}}$	$B(\mathrm{E2})_{\mathrm{SM}}$	$B(\mathrm{E2})_{\mathrm{rot}}$	$B(\mathrm{M1})_{\mathrm{exp}}$	$B(\mathrm{M1})_{\mathrm{SM}}$
$5/2^+ \to 1/2^+$	61(7)	127[a]	69[a]/114[b]	–	–
$5/2^+ \to 3/2^+$			20[a]/32[b]	0.1–0.5	0.38[a]
$3/2^+ \to 1/2^+$		106[a]	140[a]/145[b]	0.019(4)[c]	0.06[a]

[a] From Ref. [16].
[b] From Ref. [35].
[c] From Ref. [36].

the idea that for the $N = 19$ magnesium isotope not only the ground state but also excited states are no longer dominated by a spherical configuration. Although the E2 strength of the $5/2^+ \to 1/2^+$ transition in ^{31}Mg is a bit smaller it is comparable to the corresponding $2^+ \to 0^+$ transition in ^{32}Mg. The deviation can be explained by the assumption that higher lying states in ^{31}Mg are not dominated by pure intruder configurations [16,35], but contain an admixture of other particle-hole configurations.

Acknowledgements

This work has been supported by the German BMBF under contracts 06K-167, 06KY205I, and 06KY9136.

References

[1] T. Otsuka, et al., Phys. Rev. Lett. 87 (2001) 082502.
[2] T. Otsuka, et al., Eur. Phys. J. A 15 (2002) 151.
[3] R. Kanungo, et al., Phys. Rev. Lett. 102 (2009) 152501.
[4] C. Thibault, et al., Phys. Rev. C 12 (1975) 644.
[5] C. Détraz, et al., Nucl. Phys. A 394 (1983) 378.
[6] X. Campi, et al., Nucl. Phys. A 251 (1975) 193.
[7] E.K. Warburton, et al., Phys. Rev. C 41 (1990) 1147.
[8] T. Otsuka, et al., Phys. Rev. Lett. 95 (2005) 232502.
[9] P. Fallon, et al., J. Phys.: Conf. Ser. 49 (2006) 165.
[10] Y. Yanagisawa, et al., Phys. Lett. B 566 (2003) 84.
[11] P. Doornenbal, et al., Phys. Rev. Lett. 103 (2009) 032501.
[12] Y. Utsuno, et al., Phys. Rev. C 70 (2004) 044307.
[13] S. Ettenauer, et al., Phys. Rev. C 78 (2008) 017302.
[14] B.V. Pritychenko, et al., Phys. Rev. C 63 (2001) 011305.
[15] G. Neyens, et al., Phys. Rev. Lett. 94 (2005) 022501.
[16] F. Maréchal, et al., Phys. Rev. C 72 (2005) 044314.
[17] B.V. Pritychenko, et al., Phys. Rev. C 65 (2002) 061304.
[18] T. Motobayashi, et al., Phys. Lett. B 346 (1995) 9.
[19] J.A. Church, et al., Phys. Rev. C 72 (2005) 054320.
[20] H. Iwasaki, et al., Phys. Lett. B 522 (2001) 227.
[21] A. Gade, et al., Phys. Rev. Lett. 99 (2007) 072502.
[22] H. Iwasaki, et al., Phys. Lett. B 620 (2005) 118.
[23] B.V. Pritychenko, et al., Phys. Rev. C 66 (2002) 024325.
[24] V. Tripathi, et al., Phys. Rev. C 73 (2006) 054303.
[25] A.M. Hurst, et al., Phys. Lett. B 674 (2009) 168.
[26] O.T. Niedermaier, et al., Phys. Rev. Lett. 94 (2005) 172501.
[27] P. Himpe, et al., Phys. Lett. B 643 (2006) 257.
[28] D. Kameda, et al., Phys. Lett. B 647 (2007) 93.
[29] V. Tripathi, et al., Phys. Rev. Lett. 101 (2008) 142504.
[30] P. Himpe, et al., Phys. Lett. B 658 (2008) 203.
[31] B.V. Pritychenko, et al., Phys. Rev. C 63 (2001) 047308.
[32] K. Wimmer, et al., Phys. Rev. Lett. 105 (2010) 252501.
[33] G. Klotz, et al., Phys. Rev. C 47 (1993) 2502.
[34] F. Maréchal, et al., Phys. Rev. C 76 (2007) 059902E.
[35] M. Kimura, Phys. Rev. C 75 (2007) 041302.
[36] http://www.nndc.bnl.gov/ensdf/.
[37] http://isolde.web.cern.ch/ISOLDE/.
[38] D. Habs, et al., Hyperfine Interact. 129 (2000) 43.
[39] V.I. Mishin, et al., Nucl. Instr. Meth. B 73 (1993) 550.
[40] A.N. Ostrowski, et al., Nucl. Instr. Meth. A 480 (2002) 448.
[41] J. Eberth, et al., Prog. Part. Nucl. Phys. 46 (2001) 389.
[42] J. Cub, et al., Nucl. Instr. Meth. A 453 (2000) 522.
[43] W. Weinzierl, Diploma thesis, TU Munich, 2006.
[44] U. Köster, et al., Nucl. Instr. Meth. B 204 (2003) 347.
[45] C.M. Mattoon, et al., Phys. Rev. C 75 (2007) 017302.
[46] H. Mach, et al., Eur. Phys. J. A 25 (2005) 105.
[47] D. Miller, et al., Phys. Rev. C 79 (2009) 054306.
[48] T. Czosnyka, et al., Bull. Am. Phys. Soc. 28 (1983) 745.
[49] W.D. Hamilton, The Electromagnetic Interaction in Nuclear Spectroscopy, North-Holland Publishing Company, Amsterdam, Oxford, 1975.
[50] B.V. Pritychenko, et al., Phys. Lett. B 461 (1999) 322.